DOI https: //doi. org/10.1007/s11595-018-1779-y

Simulation and Experiment of Double Grits Interacting Scratch for Optical Glass BK7

ZHANG Feihu, LI Chen*, ZHAO Hang, LENG Bing, REN Lele
(School of Mechatronics Engineering, Harbin Institute of Technology, Harbin 150001, China)

Abstract: The elastic-plastic transition regime and brittle-ductile transition regime in scratch process for optical glass BK7 were analyzed based on the Hertzian equation and the stress ratio theory which was proposed by Wei. The interacting scratch process for optical glass BK7 with the grit interval distance as the variable was simulated by the ABAQUS software of finite element simulation based on the energy fracture theory. Double grits interacting scratch test for optical glass BK7 was carried out on the DMG ULTRASONIC 70-5 linear, by which the reliability of finite element simulation was verified. The surface morphology of the workpiece was analyzed by scanning electron microscopy (SEM), which showed that the width of groove increased obviously with the increase of scratch depth and the grit interval distance. Results of the width of groove were consistent with the simulation results. The subsurface damage layer was analyzed by the method of HF acid etching, which showed that there was an area of cracks intersecting. The scratching force was measured by the three-dimensional dynamometer of KISTLER, which showed that the second scratching force increased with the increase of scratching depth and the grit interval distance. The force in the second scratch was smaller than that in the first time, which was consistent with the Griffith fracture theory.

Key words: double grits interacting scratch; optical glass BK7; groove width; second scratching force

1 Introduction

Hard brittle materials such as optical glass and engineering ceramics, interesting in grinding of advanced ceramics over the last two decades, are widely used in aerospace, petrochemical industry, electrical and electronic engineering, automobile and manufacturing with their low density, chemical stability, high hardness and high strength. On the contrary, they are typical difficult-to-machine materials owing to their great hardness and low fracture toughness[1-3]. At present, grinding is the main processing method. Guo *et al*[4] presented a series of micro-structured coarse-grained diamond wheels for optical glass surface grinding aiming to improve the grinding performance, especially subsurface damage. Compared with conventional coarse-grained diamond wheel, the subsurface damage depth was reduced effectually from 5 to 1.5 μm, although the better surface roughness was not obtained by the micro-structured coarse-grained diamond wheel. Lim *et al*[5] conducted a fundamental study on the mechanism of electrolytic in-process dressing (ELID) grinding for optical glass BK7. The results showed that the cutting force was unstable throughout the grinding process due to the breakage of an insulating layer formed on the surface of the grinding wheel, while a smoother surface could be obtained using a high dressing current duty ratio at the cost of high tool wear. Yao *et al*[6] conducted surface grinding experiments for optical glass BK7 and established a relationship between the surface roughness and subsurface. It was found that the relationship between surface roughness and subsurface crack depth was influenced by the half apex angle of abrasive grain as well as the magnitude of extra grain extrusion.

Although great progress in research on hard brittle materials has been made, the removal mechanism and surface deformation characteristic of hard brittle materials are still in the exploratory stage. Nano-scratch is an effective means, which can research the material removal mechanism and the surface deformation characteristic. Many scholars research the material removal mechanism and the surface deformation characteristic based on single grit nano-scratch test, and have made

(Received: Dec. 5, 2016; Accepted: Oct. 25, 2017)

ZHANG Feihu(张飞虎): Prof.; Ph D; E-mail: zhangfh@hit.edu.cn

*Corresponding author: LI Chen(李琛): Ph D candidate; E-mail: hit_chenli@163.com

Funded by the National Key Research and Development Program of China (No.2016YFB1102204), the Major State Basic Research Development Program of China (973 Program) (No. 2011CB013202) and the National Natural Science Foundation of China (No. 51175126)

great progress and development[7-9]. However, single grit nano-scratch process cannot capture the characteristics of grinding because interactions may occur between neighboring grits and influence the process of material removal. Therefore, it is necessary to carry out interacting scratch which can represent the evolved damage better due to either grinding or abrasive machining[10,11].

Finite element simulation method (FEM) can effectively simulate distribution of the stress, strain, temperature and so on. Compared with the experiment, finite element simulation has some advantages which are not limited by time, space and test conditions. And FEM can obtain the continuously experimental result easily, reproduce the stress, and reproduce the strain within a very short period of time. Zhou *et al*[12] developed the amulti-particle micro finite element model with a random particle distribution in SiCp/Al composites using ABAQUS software. The results indicated that both the brittle fracture of SiC particles and the plastic flow of Al matrix occur in the process of the edge defected formation. The numerical results were also compared with the orthogonal cutting experimental data and were found to be in reasonable agreement. Zheng *et al*[13] have recently developed a comprehensive viscoelastic model with both normal and tangential components that compares well to the results obtained by using detailed FEM simulations. The model was an improvement on previous models because it not only was accurate but also had parameters that can be derived directly from material properties. Thepsonthi *et al*[14] provided investigations on 3-D FE modeling and simulation of micro-end milling process for Ti-6Al-4V titanium alloy. Predicted 3-D chip flow and shapes were compared against the experiments which provided reasonably good agreements. In addition, a comparison between 3-D and 2-D FE simulations provided gave a better understanding of utilizing their predictions.

In this paper, the finite element simulation of double grits interacting scratch was designed, and the influence of the different grit interval distances, distribution of strain and stress on surface and subsurface for width of the groove were studied. Double grits interacting scratches test for optical glass BK7 was carried out based on the simulation. The surface and subsurface morphology of the workpiece and width of the groove were analyzed by SEM. The force of scratching was measured by a three dimensional dynamometer of KISTLER. Furthermore, the influences of scratching depth and grit interval distance on the second scratching force were analyzed, by which the reliability of finite element simulation was verified.

2 Material removal mechanism

At the very beginning of the loading, there will be elastic deformation on the surface of workpiece. So the Vickers indenter can be considered to be in contact with the workpiece in the form of a spherical surface because the contact depth is very shallow. Fig.1 is the schematic diagram of contact between the indenter and workpiece. P is the normal load, R is the radius of the indenter, a is the radius of the contact area, h_t is the indentation depth, and h_c is the depth of the contact area. Within the elastic regime, h_t is equal to $2\times h_c$ for elastic response penetration[15].

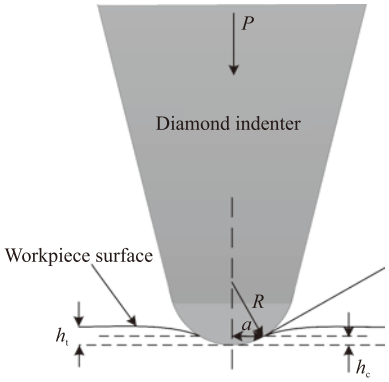

Fig.1 Schematic diagram of contact between indenter and workpiece

The projection area of the contact area in the normal direction between the indenter and the workpiece is:

$$A=\pi a^2=\pi\left(2Rh_c-h_c^2\right) \tag{1}$$

According to the Hertzian[15] equation for elastic contact of an elastically isotropic material, the relationship among the indentation depth h_t, the elastic modulus of the materials and the normal pressure P is obtained:

$$h_t=\left(\frac{9}{16}\cdot\frac{1}{R}\right)^{\frac{1}{3}}\left(\frac{P}{E_r}\right)^{\frac{2}{3}} \tag{2}$$

where E_r is the reduced elastic modulus within the elastic range, which can be calculated by considering the compliance of the workpiece and the indenter tip combined in series[15]:

$$\frac{1}{E_r}=\frac{1-\nu^2}{E}+\frac{1-\nu_i^2}{E_i} \tag{3}$$

where E_i is the elastic modulus of diamond indenter, E is the elastic modulus of workpiece, v_i is Poisson's ratio of diamond indenter and v is Poisson's ratio of work-

piece. For the diamond indenter, E_i =1 140 GPa and ν_i =0.07, for the optical glass BK7, E=81.3 GPa and ν= 0.209.

Based on Eq.1-Eq.3, the average compressive stress of the indenter is represented by the normal pressure:

$$P_m=\frac{P}{A}=\frac{4E_r h_t^{\frac{3}{2}}R^{\frac{1}{2}}}{3\pi\left(2Rh_c-h_c^2\right)}=\frac{4E_r}{3\pi}\frac{h_t}{h_c}\frac{\sqrt{h_tR}}{2R-h_c} \tag{4}$$

Approximate value of average pressure stress is obtained by assuming the h_t as the approximation a^2/R for $h_t<<R$[16]:

$$P_m\approx\frac{4E_r}{3\pi}\frac{a}{R} \tag{5}$$

From the reference[17], the value of maximum contact stress is 3/2 times as large as that of average compressive stress:

$$P_{max}=\frac{3}{2}P_m=\frac{3}{2}\frac{4E_r}{3\pi}\frac{a}{R}=\frac{2E_r a}{\pi R}\approx 1.6\frac{H}{2.8} \tag{6}$$

where H is the micro-hardness, which is measured to be 7.15 GPa.

The critical depth of elastic-plastic transition z_c[16] is:

$$z_c=0.48a=0.48\frac{P_{max}\pi R}{2E_r}=0.137\,1\frac{\pi HR}{E_r} \tag{7}$$

Wei[18] proposed the ratio of critical strain energy density by distortional deformation over that by volumetric deformation as a material parameter to quantify the ductile-to-brittle transition in glass. For mode I crack, the maximum shear stress for all θ occurs when θ=103.8°. When τ_c/p_c is bigger than τ_{max}/p_{max}, the material is brittle like, and when τ_c/p_c is smaller than τ_{max}/p_{max}, the material would be ductile like:

$$\frac{\tau_{max}}{p_{max}}=\frac{3\cos\left(\frac{\theta}{2}\right)\sqrt{(3-\cos\theta)-(1-\cos\theta)}}{4(1+\nu)} \tag{8}$$

3 Finite element simulation

3.1 Conceptual design of finite element simulation

The fracture criterion of GFI, which is based on the energy fracture theory of Brittle Crack is chosen in the simulation process because the optical glass BK7 is a kind of hard brittle material. The simulation process is performed under the dynamic explicit analysis of ABAQUS. In order to reduce the computation quantity and the dense grid, the size of workpiece in finite element simulation is chosen as 500 μm×400 μm×150 μm. The diamond Vickers indenter, whose length chisel edge is less than 1 μm and the angle is 136°, is chosen in the scratch process. As is shown in Fig.2, the finite element simulation of interacting scratch for optical glass BK7 is designed in different kinds of grit interval

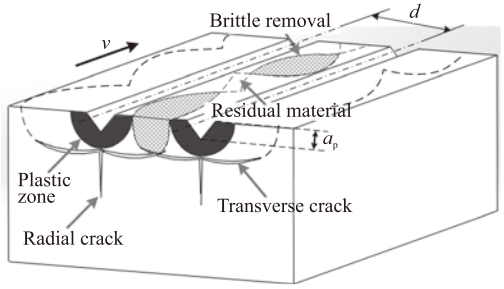

Fig.2 Schematic of interacting scratch for double grits

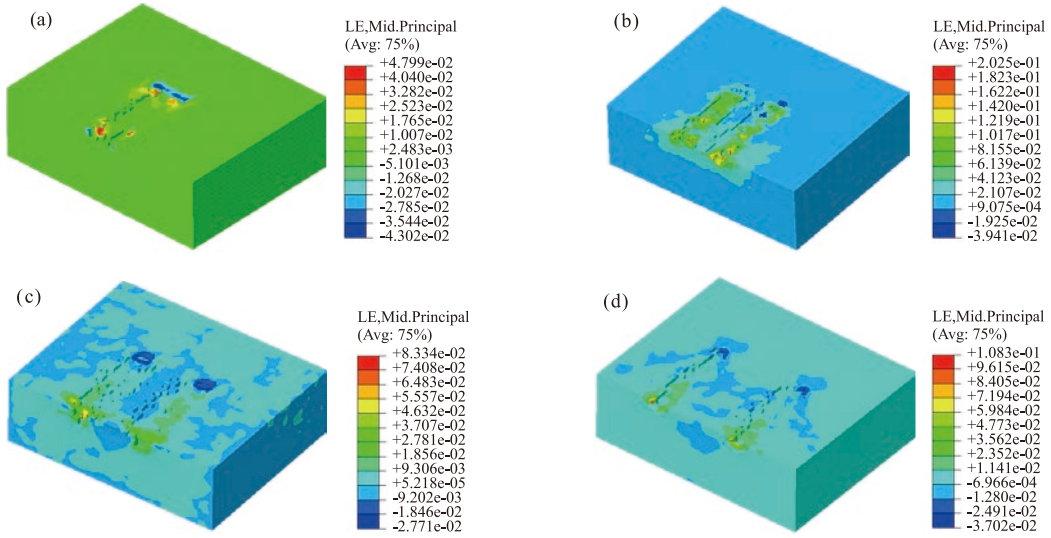

Fig.3 Surface morphology and strain distribution of workpiece for finite element simulation: (a) d=50 μm; (b) d=100 μm; (c) d=150 μm; (d) d=200 μm

distance, namely d=50 μm, d=100 μm, d=150 μm and d=200 μm. The scratch speed is 1.67 mm/s and the scratch depth is 8 μm.

3.2 Result and discussion of finite element simulation

3.2.1 Surface morphology and strain distribution of interacting scratch for finite element simulation

The three-dimensional morphology and strain distribution of the surface are shown in Fig.3, and there is an obvious area of interacting removal on the surface. The effect of interacting removal is obvious when the grit interval distances are 150 and 200 μm, while the effect of interacting removal is not obvious when the grit interval distances are 50 μm and 100 μm. The absolute value of the strain is the maximum at the contact point between the abrasive tip and the workpiece.

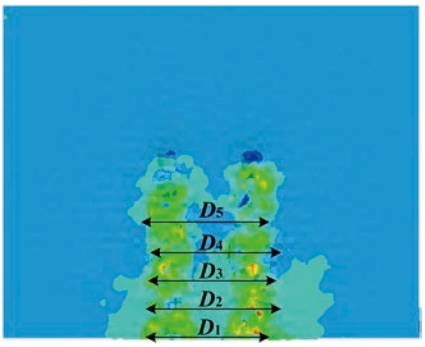

Fig.4 Schematic of groove width

As shown in Fig.4, when the influence of grit interval distance on groove width is researched, the average value of 5 samples is chosen as the groove width because the groove width is not constant in the process of scratch. The groove width is expressed as Eq.(9):

$$D=\frac{\sum_{n=1}^{5}D_i}{5} \tag{9}$$

As shown in Fig.5, the groove's width increased obviously with the increase of the grit interval distance.

3.2.2 Stress distribution on subsurface

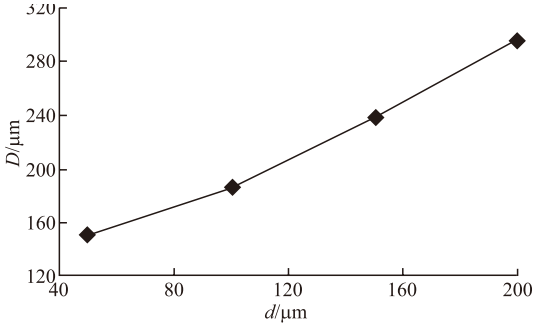

Fig.5 Influence of grit interval distance on groove width

The stress distribution on subsurface is shown in Fig.6. There's the obvious intersecting stress on the subsurface when the grit interval distances are 50 μm and 100 μm. The maximum value of intersecting stress is 8.871-11.09 GPa when the grit interval distance is 50 μm, 3.699-5.549 GPa when the grit interval distance is 100 μm, and less than 2.067 GPa when the grit interval distances are 150 and 200 μm. The larger the maximum value of intersecting stress is, the more obvious the material removal of grit interacting is.

4 Experimental device and condition

The size of workpiece, optical glass BK7, is 20 mm×20 mm×20 mm. In order to remove the glass damage layer, the surface of the workpiece is traditionally polished (the polishing powder is Cerium Oxide). The surface roughness of the polished workpiece is detected by atomic force microscopy(70 μm×70 μm), the value of which is 2 nm(Fig.7).

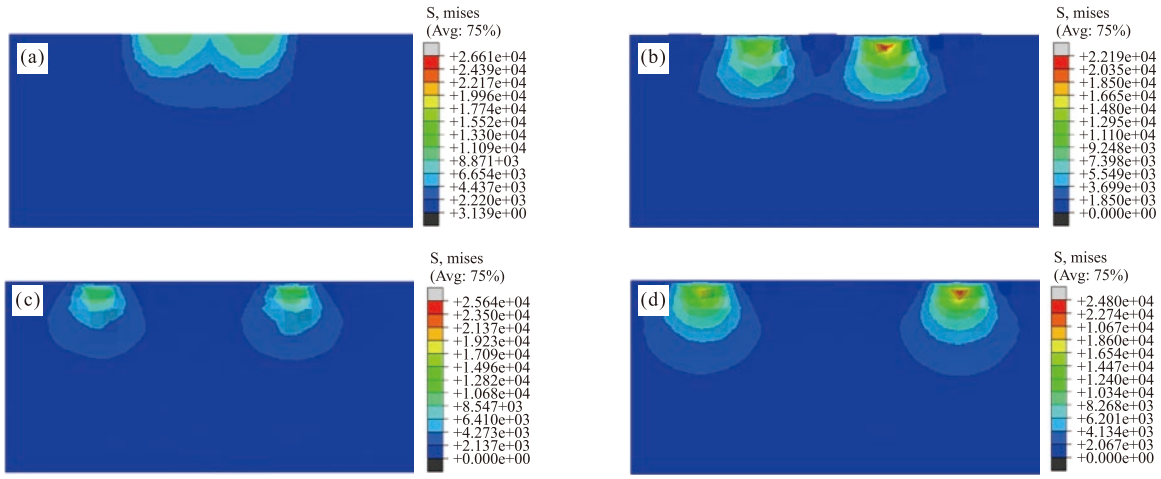

Fig.6 Stress distribution of subsurface: (a) d=50 μm; (b) d=100 μm; (c) d=150 μm; (d) d=200 μm

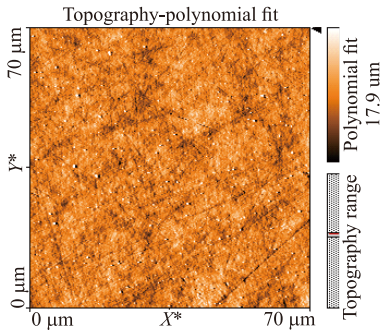

Fig.7 Atomic force microscopy of the polished workpiece

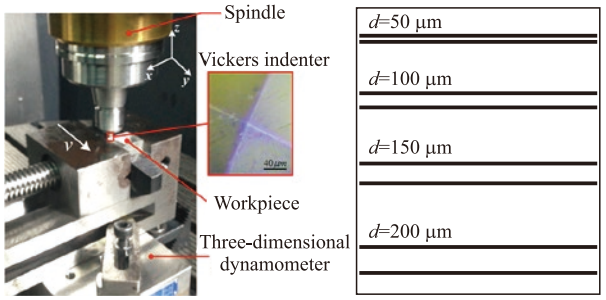

(a) Experiment device (b) Schematic diagram of scratch

Fig.8 Experimental device and condition of interacting scratch for optical glass BK7

Table 1 Experimental condition of interacting scratch

Condition No.	d/μm,	a_p/μm
1-4	50, 100, 150, 200	4
5-8	50, 100, 150, 200	6
9-12	50, 100, 150, 200	8
13-16	50, 100, 150, 200	10

As is shown in Fig.8(a), the scratch experiment for optical glass BK7 is carried out on the DMG ULTRASONIC 70-5 linear, and the scratch force is measured by three-dimensional dynamometer of Kistler. The length chisel edge for diamond Vickers indenter is less than 1 μm, and the angle is 136°(±15'). The workpiece coordinate is established by using the three point leveling system of machine tool. The speed of scratching is 100 mm/min. There is no fluid cooling in scratching because of the small scratching depth and low scratching speed. The scratch process is divided into two steps. The first step is scratching the first scratch, and the second step is scratching the second scratch where it is from the first one at the interval distance of d.

As shown in Fig.8(b), the experiment of interacting scratch for optical glass BK7 is designed in different grit interval distances, namely d=50, 100, 150 and 200 μm. There're four times scratches in each workpiece. What's more, to explore the influence of scratch depth on the material removal and scratch force, the experiment of interacting scratch for optical glass BK7 is designed in different kinds of scratch depths, namely a_p=4, 6, 8, and 10 μm. The specific test conditions are shown in Table 1.

5 Result and discussion

5.1 Surface morphology of interacting scratch

The three dimensional morphology of the surface of glass was observed by Hitachi SU8010 scanning electron microscope (SEM). The workpiece was treated by spraying-gold before observed by SEM because the optical glass BK7 was an insulator. As shown in Fig.9, the surface morphology of groove was observed by SEM. The chunk removal(black arrow) and segmented chips(dotted circle) were found on the groove surface, which were the main forms of material removal. And there were obvious residual materials(White arrow) on the surface. The fracture form of the groove edge was formed mainly by the shell-shaped fracture, and the scratch edge was sharp wedge. What's more, because the growth direction of crack which is influenced by the shear stress is perpendicular to the direction of shear stress, the included angle between the direction of fracture and the direction of scratch is about 45°. There were transverse cracks extended to the surface in groove edge(Full line ellipse). While there was an interacting area, the interacting effect of transverse

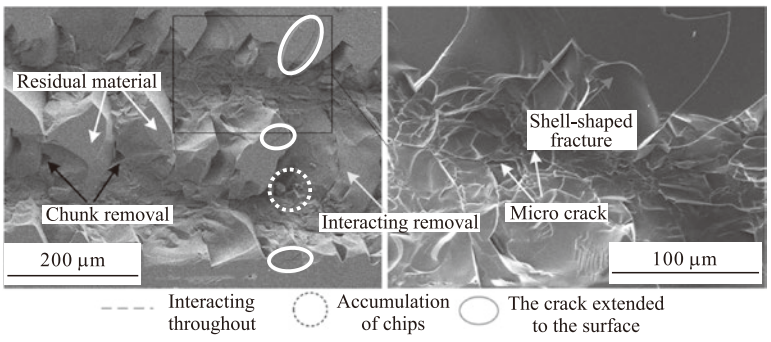

Fig. 9 Interacting removal of groove morphology

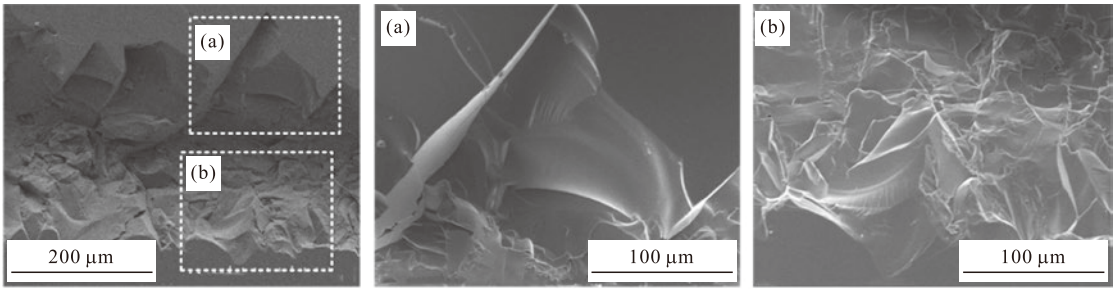

Fig.10 Comparison of the groove boundary in the first scratch and the second scratch

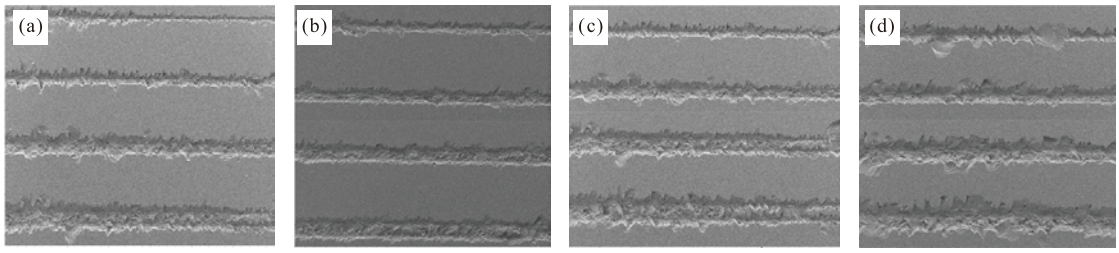

Fig.11 Comparison of groove morphology with different scratch conditions: (a) a_p=4 μm; (b) a_p=6 μm; (c) a_p=8 μm; (d) a_p=10 μm

cracks extended to the surface leading to the interacting removal of material. The radial cracks were caused by the normal scratch force, and a large amount of micro cracks in the groove's surface were caused by the process of unloading.

As shown in Fig.10, we find that there is almost no residual material between the two grooves when the grit interval distance is small enough, and the residual boundary of the second scratch is better than that of the first time. (Fig.10(a) is the first scratch and Fig.10(b) is the second scratch).

The groove morphology in different kinds of depth and different kinds of grit interval distance is shown in Fig.11, which shows that the width of groove increased obviously with the increase of scratch depth and the increase of grit interval distance. The effect of interacting removal was obvious when the grit interval distances were 150 and 200 μm, and was not obvious when the grit interval distances were 50 and 100 μm, which was consistent with the simulation result.

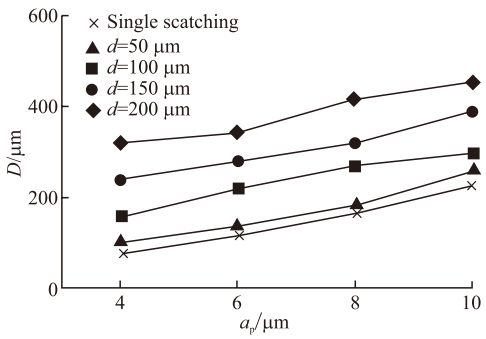

Fig.12 Relationship between groove width and scratch depth

After cleaning the workpiece by ultrasonic cleaning machine, the value of groove width was measured by confocal scanning laser microscope OLS3000. The average value of 5 samples was chosen as the groove width because the groove's width was not constant in the scratch process. As shown in Fig.12, the groove's width increased obviously with the increase of scratch depth. As shown in Fig.13, the groove's width increased obviously with the increase of grit interval distance, which was consistent with the simulation result.

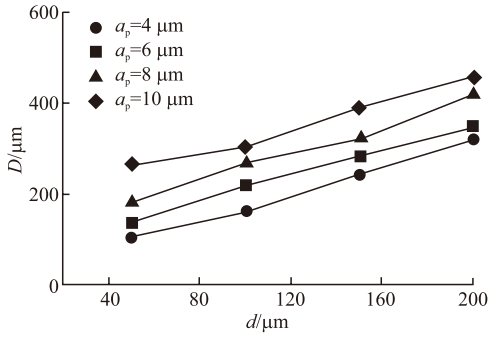

Fig.13 Relationship between groove width and interval distance

5.2 Analysis of subsurface crack in interacting scratch

Subsurface cracks will affect the strength and long-term stability of optical components directly, so it is important to study the subsurface cracks in the process of interacting scratch[19]. As shown in Fig.14(a), the scratch cross section was polished to a mirror(the roughness is about 2 nm) by using the traditional polishing technology(polishing powder is cerium oxide), and the subsurface morphology of the scratch cross section was observed by SEM. The polished cross section was treated by the method of HF acid etching to observe the subsurface cracks clearly. In order to reduce the effect of corrosion on the surface damage

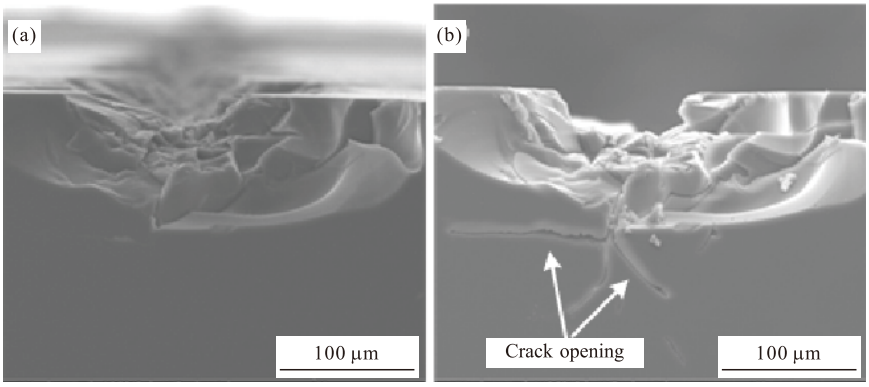

Fig.14 Comparison of subsurface morphology before and after etching

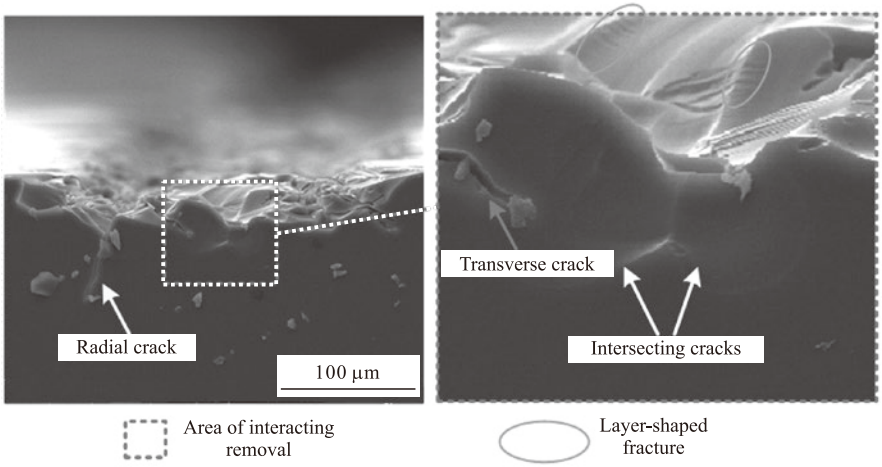

Fig.15 Subsurface morphology of scratch

for optical glass BK7, the HF acid solution was diluted from 40% to 1%, and the workpiece was immersed in diluted solution for 10 min. As shown in Fig.14(b), the subsurface after HF acid etching was cleaned by ultrasonic cleaning machine. The subsurface morphology of the workpiece before corroding was consistent with that after corroding. The subsurface cracks of the workpiece was opened by HF acid only, and there was no other damage to the cross section.

As shown in Fig.15, there're typical radial and transverse cracks on the subsurface, and particularly the layer-shaped cracks appeared in the workpiece due to the uneven distribution of stress. And there was obvious intersecting crack on the subsurface, which described the distribution of subsurface cracks in the grinding process more explicitly than the single grit scratch.

5.3 Analysis of normal scratch force

The change of the scratch force is closely related to factors in the process of scratch, which is the characterization of indenter acting on the surface of workpiece under load condition. Due to the interaction between single diamond and specimen in the process of static scratch, there would be plastic deformation, elastic deformation, brittle fracture, material removal, and other forms of damage in the process of optical glass BK7, resulting in the scratch force altering with the change of scratch factors. In the process of scratch, axial force is mainly related to swing of rotating grinding wheel, and tangential force mainly affects indenter wear and machine tool's power consumption. Normal force is the most important parameter related to the deformation and surface quality of the workpiece. So in this paper, we only took the normal force into consideration in the process.

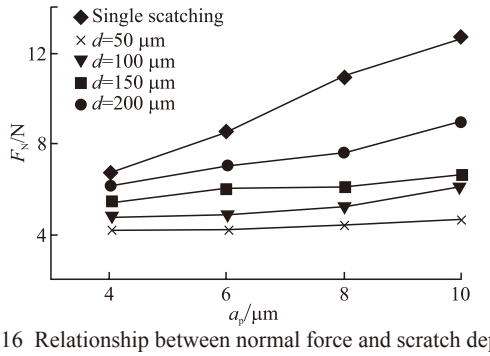

Fig.16 Relationship between normal force and scratch depth

As shown in Fig.16, the force in the second scratch is smaller than that in the first time. With the increase of scrach depth, it is influenced by the damage caused by the new transverse cracks in first scrach.

According to the Griffith fracture theory[20](Eq. 10), the length of crack radius for new transverse cracks is longer than that before the first scratch, which results in the fracture stress reducing and the low stress fracture. And it's found that the second scratch force increased with the increase of scratch depth:

$$\sigma_{\text{crit}} = \sqrt{\frac{2E'r^s}{\pi c}} \tag{10}$$

where σ_{crit} is the Griffith fracture stress, r^s is the surface energy of the new surface in fracture process, c is the length of crack radius, and E' is the elasticity modulus.

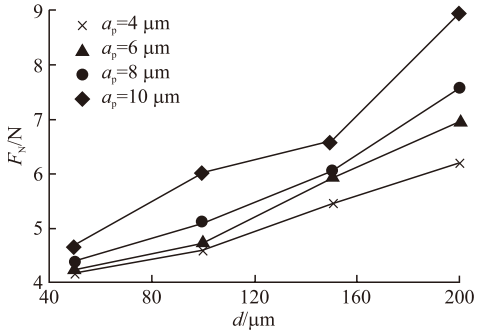

Fig.17 Relationship between normal force and interval distance

As is shown in Fig.17, with the increase of grit interval distance, the interacting effect is gradually weakened and the scrach force in the second scrach is gradually becoming smaller ,which is gradually getting closer to that in the first time.

6 Conclusions

The interacting scratch process for optical glass BK7 with the grit interval distance as the variable was simulated by the ABAQUS software of finite element simulation based on the energy fracture theory Brittle Crack. Double grits interacting scratch test for optical glass BK7 was carried out on the DMG ULTRASONIC 70-5 linear. And some conclusions were obtained through this investigation:

a) The surface morphology of the workpiece was analyzed by SEM. The results showed that the groove's width increased obviously with the increase of scratch depth and the grit interval distance, which was consistent with the simulation results.

b) The subsurface damage layer was analyzed by the method of HF acid etching. It was found that there was an area of cracks intersecting, which described the distribution of subsurface crack in the grinding process more explicitly than the single grit scratch.

c) The scratch force was measured by the three dimensional dynamometer of KISTLER, which showed that the second scratch force increased with the increase of scratch depth and the grit interval distance. The force in the second scratch was smaller than that in the first time, which was consistent with the Griffith fracture theory.

References

[1] Chen X, Ma L, Li C, *et al*. Experiment Study and Genetic Algorithm-based Optimization of Cutting Parameters in Cutting Engineering Ceramics[J]. *Int. J. Adv. Eng. Tech*., 2014,74(5-8): 807-817

[2] Chen J, Fang Q, Li P. Effect of Grinding Wheel Spindle Vibration on Surface Roughness and Subsurface Damage in Brittle Material Grinding[J]. *Int. J. Mach. Tool. Manu*., 2015, 91:12-23

[3] Li C, Zhang F, Meng B. Material Removal Mechanism and Grinding Force Modelling of Ultrasonic Vibration Assisted Grinding for SiC Ceramics[J]. *Ceram. Int*., 2017, 43(3): 2 981-2 993

[4] Guo B, Zhao Q, Fang X. Precision Grinding of Optical Glass with Laser Micro-structured Coarse-grained Diamond Wheels[J]. *J. Mater. Process. Tech.*, 2014, 214: 1 045-1 051

[5] Lim H S, Fathima K, Kumar A S. A Fundamental Study on the Mechanism of Electrolytic In-process Dressing (ELID) Grinding[J]. *Int. J. Mach. Tool. Manu.*, 2002, 42: 935-943

[6] Yao Z, Gu W, Li K. Relationship between Surface Roughness and Subsurface Crack Depth during Grinding of Optical Glass BK7[J]. *J. Mater. Process. Tech.*, 2012, 212: 969-976

[7] Meng B, Zhang F, Li Z. Deformation and Removal Characteristics in Nanoscratching of 6H-SiC with Berkovich Indenter[J]. *Mat. Sci. Semicon. Proc.*, 2015, 31:160-165

[8] Li C, Zhang F, Ding Y. Surface Deformation and Friction Characteristic of Nano Scratch at Ductile-removal Regime for Optical Glass BK7[J]. *Appl. Optics*, 2016, 55(24): 6 547-6 553

[9] Fang T, Chang W, Lin C. Nanoindentation and Nanoscratch Characteristics of Si and GaAs[J]. *Microelectron. Eng*., 2005, 77: 389-398

[10] Klecka M, Subhash G. Grain Size Dependence of Scratch-induced Damage in Alumina Ceramics[J]. *Wear*, 2008, 263: 137-148

[11] Xu H H K, Jahanmir S, Wang Y. Effect of Grain Size on Scratch Interactions and Material Removal in Alumina[J]. *J. Am. Ceram. Soc*., 1995, 78: 881-891

[12] Zhou L, Wang L, Ma Z Y. Finite Element and Experimental Studies of the Formation Mechanism of Edge Defects during Machining of SiCp/Al Composites[J]. *Int. J. Mach. Tool. Manu*., 2014, 84: 9-16

[13] Zheng Q J, Zhu H P, Yu A B. Finite Element Analysis of the Contact Forces between a Viscoelastic Sphere and Rigid Plane[J]. *Powder Technol.*, 2012, 226:130-142

[14] Thepsonthi T, Özel T. 3-D Finite Eelement Process Simulation of Micro-end Milling Ti-6Al-4Vtitanium Alloy: Experimental Validations on Chip Flow and Tool Wear[J]. *J. Mater. Process. Tech.*, 2015, 221: 128-145

[15] Hertz H, Jones D E, Schott G A. *Miscellaneous Papers*[M]. London: Macmillan and Company, 1896

[16] Tabor D. *The Hardness of Metals*[M]. Oxford: Clarendon Press, 1951

[17] Lee S H. Analysis of Ductile Mode and Brittle Transition of AFM Nanomachining of Silicon[J]. *Int. J. Mach. Tool. Manu*., 2012, 61: 71-79

[18] Yujie Wei. The Intrinsic and Extrinsic Factors for Brittle-to-ductile Transition in Bulk Metallic Glasses[J]. *Theor. Appl. Fract. Mec*., 2014, 71: 6-78

[19] Li S, Wang Z, Wu Y. Relationship between Sub-surface Damage and Surface Roughness of Optical Materials in Grinding and Lapping Processes[J]. *J. Mater. Process. Tech*., 2008, 205(1): 34-41

[20] Griffith A A. The Phenomena of Rupture and Flow in Solids[J]. *Philosophical Transactions of the Royal Society of London. Series A, Containing Papers of a Mathematical or Physical Character*, 1921, 221: 163-198